Scripta Materialia 242 (2024) 115965

Contents lists available at ScienceDirect

Scripta Materialia

journal homepage: www.journals.elsevier.com/scripta-materialia

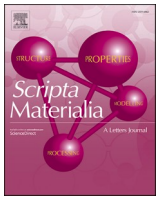

On the influence of crystallographic texture on cyclic hardening of an AlMgSi alloy

Akash Gopal, Sohail Shah, Bjørn Holmedal *

Department of Material Science and Engineering, Norwegian University of Science and Technology (NTNU), Trondheim, 7491, Norway

ARTICLE INFO

Keywords:
Aluminum alloys
Cyclic ageing
Dynamic strain ageing
Texture
Cumulative plastic strain

ABSTRACT

The influence of crystallographic texture on hardening achieved by cyclic loading at room temperature, was tested by comparing samples from an axisymmetric round bar and a flat profile, both made of non-recrystallized, extruded profiles of similar AlMgSi alloys (AA6082). It was found that the plastic strain accumulated during the cyclic loading was significantly (nine times) larger for the flat profile. Tensile testes of the cyclically hardened samples revealed that in spite of the large accumulated plastic strain during cyclic hardening of the flat sample, the local tensile strain at fracture in the necking region was similar to the peak aged conditions obtained by artificial aging.

AlMgSi alloys derive strength from precipitation of second phase particles in the aluminum matrix, traditionally achieved by a solution heat treatment followed by quenching and either natural or artificial aging. Recently, a new technique of strengthening heat treatable AlCu, AlMgSi and AlZnMg aluminum alloys, by cyclic loading at room temperature, was reported to provide similar strength and uniform elongation as the peak aged artificially aged conditions [1–5]. Recent studies of AlZnMg alloys [3,4] have shown that the solute clusters formed during cyclic aging resemble the GP zones formed during natural aging of the alloy. The detailed structure of the clusters/zones formed during cyclic aging of AlMgSi alloys, has not been characterized in detail yet.

The cyclic aging process imposes a plastic strain on the material during each cycle. This plastic strain accelerates the precipitation at room temperature by enhanced substitutional diffusion that provides the required vacancies, assumingly formed by dragging of jogs on screw dislocations [5]. However, with each cycle, the plastic strain imposed on the material being processed, accumulates [4]. Plastic strain accumulation during processing may therefore potentially degrade the ductility of the cyclic hardened material by low-cycle fatigue.

In the current investigation, the influence of the texture on the accumulation of plastic strain during cyclic aging and the influence of the plastic strain on the fracture strain and mode are investigated.

A flat extrusion of AA6082, referred to as AA6082-flat, and an axisymmetric AA6082 extrusion, referred to as AA6082-round are considered. The AA6082-flat alloy had a profile thickness of 6 mm, width of 40 cm and was delivered by Benteler Automotive. The texture was a typical rolling texture with a strong beta fiber characterized by strong $\{112\}\langle 11\bar{1}\rangle$ (Copper), $\{011\}\langle 21\bar{1}\rangle$ (Brass) and $\{123\}\langle 63\bar{4}\rangle$ (S) texture components, which can be recognised in the 111 pole figure in Fig. 1a. The AA6082-round had a profile diameter of 50 mm and was delivered by Norsk Hydro Aluminium. The axisymmetric texture was dominated by the $\langle 111\rangle$ and $\langle 100\rangle$ fibres as seen in the inverse pole figure in Fig. 1b. The chemical compositions of the two alloys are given in Table 1.

To avoid buckling during cyclic aging, relatively thick and short samples were cut parallel to the extrusion direction for both AA6082-flat and AA6082-round, with dimensions as shown in Fig. 2. A square cross section with a thickness of 6 mm was used for the cyclic hardening as well as for all tensile tests of both AA6082-flat and AA6082-round. Solutionizing heat treatment of the tensile samples were performed in a salt bath, for AA6082-flat at 525 °C for 30 min and for AA6082-round at 560 °C for 10 min, after which the samples were quenched in cold water immediately.

The peak aged conditions were obtained based on the recommendations of the material suppliers: 525 °C at 30 min for AA6082-flat and 560 °C at 10 min for AA6082-round. Cyclic aging tests were performed according to procedures used in [5], gradually increasing the stress amplitude in each cycle until a prescribed targeted stress, σ_t, is reached. The number of cycles, N, to reach this targeted stress is specified. Additionally, the time per cycle is prescribed. At any cycle, n, the stress amplitude can be expressed

* Corresponding author.
E-mail address: bjorn.holmedal@ntnu.no (B. Holmedal).

https://doi.org/10.1016/j.scriptamat.2023.115965
Received 19 November 2023; Received in revised form 13 December 2023; Accepted 30 December 2023

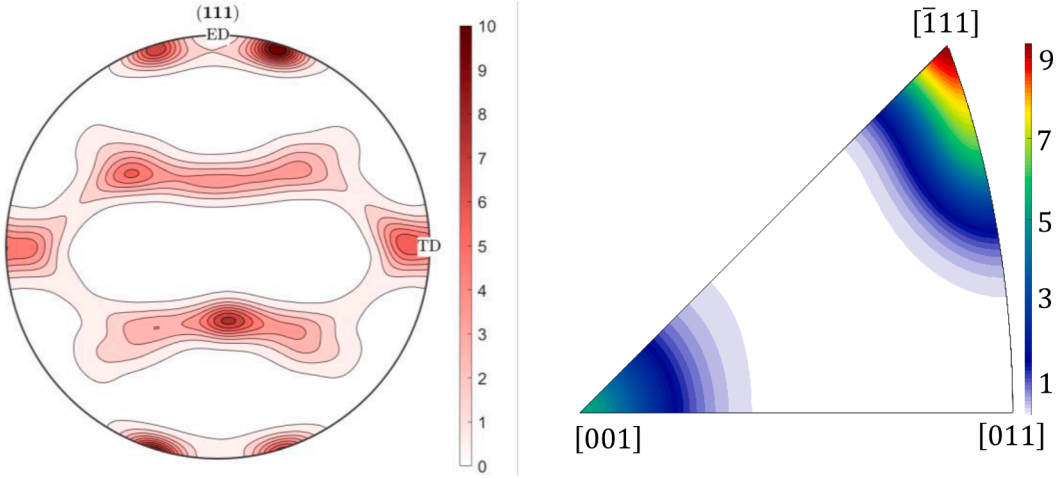

Fig. 1. a) 111 pole figure for AA6082-flat and b) inverse pole figure for AA6082-round.

Table 1
Chemical Composition, in wt%.

Material	Al	B	Cr	Cu	Fe	Mg	Mn	Si	Ti	V	Zn
AA6082-flat	97.4	0.004	0.16	0.01	0.21	0.65	0.52	0.91	0.02	0.02	0.06
AA6082-round	96.9	–	0.18	0.08	0.24	0.75	0.60	1.20	–	–	–

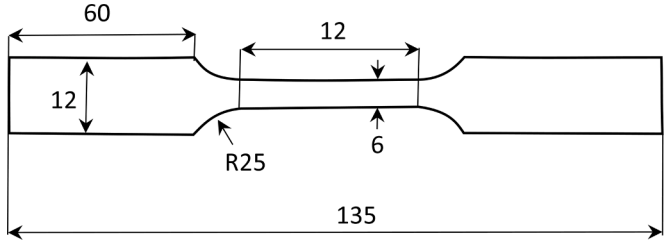

Fig. 2. Sample geometry for cyclic aging tests. All dimensions are in mm.

$$\sigma_n = \sigma_0 + (\sigma_t - \sigma_0)\sqrt{\frac{n}{N}} \quad (1)$$

Here, σ_0 is the initial stress amplitude, corresponding to the nominal yield strength of the as-solutionized and water quenched state of the alloy. The cyclic aging tests were conducted on an Instron 250 kN axial servo-hydraulic fatigue test machine. A more detailed description of the setup can be found in [3].

The load during cyclic aging was given by a sinusoidal function, as described in reference [3]. The strains during the tests were measured using digital image correlation, and the accumulated plastic strain was estimated, also described in detail in reference [3].

The nominal strain rate for the uni-axial tensile tests was set to 0.0014 s^{-1} for all final tests of the materials. Fracture surface analysis was conducted using secondary electron mode in a Zeiss Supra Field Emission scanning electron microscope with an accelerating voltage of 15 kV, keeping as large working distance as possible. The textures were measured by coarse EBSD scans on a polished+electropolished 16 mm^2 region of the cross section of the tensile tests using a Zeiss Ultra 55 using a NORDIF UF1100 detector. The projected cross-sectional area of the final fracture surface was measured using Stereo Microscopy.

Cyclic aging tests were conducted at different frequencies, targeted stress, and number of cycles for AA6082-round in a similar investigation as the one reported for two AlZnMg alloys in reference [3]. From these results, it was found that processing at a targeted peak stress of 300 Mpa in 420 cycles at 5 s per cycle was the optimum set of processing parameters amongst those tested to obtain appreciable nominal tensile strength and uniform strain. The cumulative plastic strain after cyclic aging of AA6082-round was 52 %. A description of how to calculate the cumulative plastic strain from the cyclic stress-strain curves can be found in [3]. The nominal stress-strain curve from a tensile test of this material is shown in Fig. 3, along with curves for the peak aged condition and for the solutionized and quenched condition.

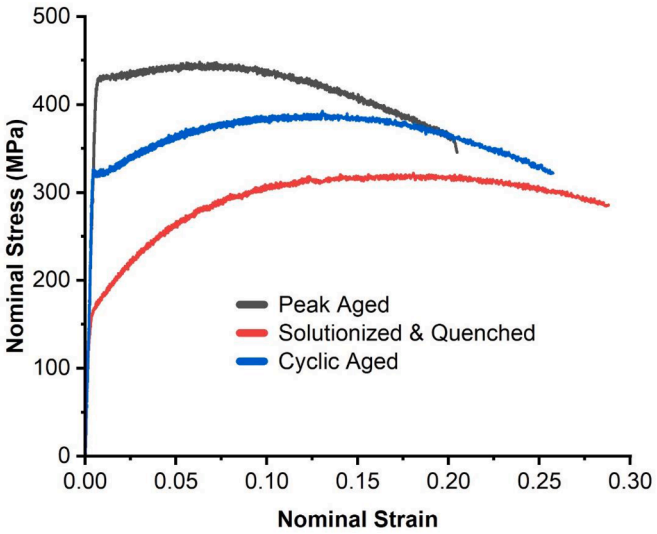

Fig. 3. Nominal stress versus strain curves for the cyclic aged condition, the peak aged condition and the solutionized and quenched condition for AA6082-round.

Diffuse necking was observed for tensile tests of solutionized and quenched, for peak aged and for cyclic aged AA6082-round. The local fracture strain in the neck, as calculated from the decrease of the cross-sectional area from the initial A_0 to the projected fracture area A_f, is similar for the cyclic aged and the artificially aged conditions.

For the AA6082-flat, the same number of cycles and the same time per cycle was used as for AA6082-round. It was compensated for the

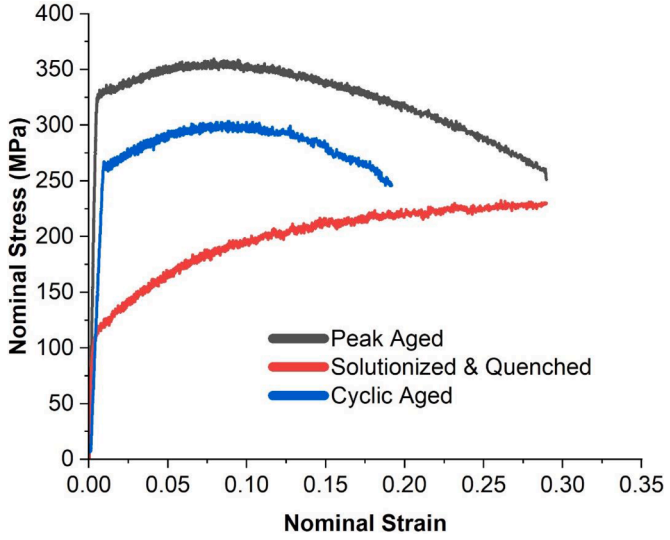

Fig. 4. Nominal stress versus strain curves for the cyclic aged condition, the peak aged condition and solutionized and quenched condition for AA6082-flat.

different textures and correspondingly different Taylor factors, by that the targeted stress for the AA6082-flat was set equal to approximately the same percentage of the nominal tensile strength as for the AA6082-round (250MPa). This also compensates for the slightly different chemical compositions.

The cumulated plastic strain during cyclic aging of the AA6082-flat was 471 %, which is significantly larger than for AA6082-round. The difference between these alloys is mainly the texture, with orthotropic versus axi-symmetric symmetry. A similarly high cumulative plastic strain for specimens made from flat extrusions, has earlier been reported for AlZnMg alloys [3]. Hence, the reason for the difference is likely to be the high number of symmetric slip systems being activated during tensile testing of the axisymmetric texture components. The ⟨100⟩ fiber orientations have eight symmetric active slip systems and the ⟨111⟩ fiber orientations have six symmetric active slip systems. Amongst the major beta fiber components of the flat extrusion samples, the Copper orientations also have six symmetric slip systems during the tensile tests, but the Brass orientations have only two and the S orientations have only one slip system with the highest Schmid factor. It is reasonable to assume that with more slip systems active, more jogs are generated due to more dislocation interactions, providing more vacancies for the accelerated precipitation.

Plots of nominal stress versus strain for the solutionized and quenched condition, the peak aged condition and the cyclic aging

Table 2
True fracture strain values for AA6082-round.

Sample	True fracture strain (%) $\varepsilon_f = \ln(A_0/A_f)$
Solutionized & Quenched	32
Peak Aged	35.5
Cyclic Aged	35.3

condition are compared in Fig. 4. The solutionized and quenched condition contains Mg and Si in solid solution. These are alloying elements which are known to give dynamic strain aging in aluminum alloys. The serrations seen on the tensile curve can be explained by the occurrence of the Portevin Le Chatelier instability. An early slant shear fracture occurred in this tensile test at around maximum force. This fracture mode, where the specimen is sheared in two by a 45° cut, is very similar as reported by Chung et al. [6]. In their work, dynamic strain aging was concluded as the origin also for early slant shear fracture in solutionized and quenched condition for an AlZnMg alloys [6] and is believed to be the reason for this fracture mode also here. Interestingly, this fracture mode occurred only for AA6082-flat and not for the samples with axi-symmetric texture, which experienced a classical cup-and-cone fracture. It is reasonable to assume that an interplay between the texture and the flow localization due to the strain rate softening caused by dynamic strain aging is responsible for the shear-fracture mode in the solutionized and quenched condition.

However, both the peak aged and the cyclic aging conditions show a considerable amount of necking. The fracture strains in the necking zone are listed in Table 3. Both the fracture strain of the cyclic aged condition and of the artificially aged AA6082-flat alloy are larger than for AA6082-round.

For the case of flat extruded AlZnMg alloys, Shah et al. [3] reported early slant fractures occurring at maximum load in tensile tests, as an alternative to diffuse necking for cyclic aged specimens. Also, they ruled out dynamic strain aging or damage as reasons for this, by analysing low-temperature tests and artificial aging of cyclic aged samples. However, diffuse necking behavior and good ductility were reported in the work by Sun et al. [5], who investigated cyclic aged axisymmetric samples, including both AlZnMg and AlMgSi alloys. Hence, one could suspect that the texture is important for the early slant fracture to occur. However, early slant fracture did not occur in the cyclic aged AA6082-flat.

Secondary electron SEM observations were made on the fracture surfaces of cyclic aged AA6082-round and AA6082-flat, as illustrated in Fig. 5. It was observed predominantly ductile fracture modes with presence of dimples on the fracture surfaces. Since fracture occurs in the non-uniform necking deformation, the fracture strain based on the elongation of the extensometer depends on the choice of extensometer,

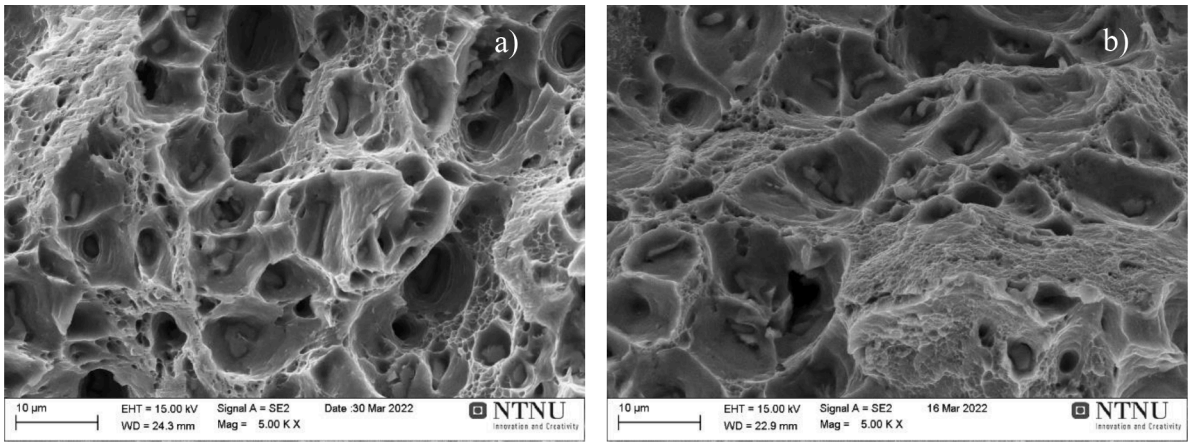

Fig. 5. Selected SEM images of fracture surfaces of cyclic aged a) AA6082-flat, b) AA6082-round.

Table 3
True fracture strain values for AA6082-flat.

Sample	True fracture strain (%) $\varepsilon_f = \ln(A_0/A_f)$
Solutionized & Quenched	24.8
Peak Aged	66.4
Cyclic Aged	54.3

how centered the necking region is as compared to the extensometer and on the sample geometry. Hence, it does not give a precise measure of the ductility. Instead, the true fracture strain was estimated based on the projected fracture surface. Interestingly, as can be read from Tables 2 and 3 the fracture strain is largest for AA6082-flat, even though the cumulated plastic strain is much larger. For both alloys, the fracture strain is similar as for the peak aged condition obtained by artificial aging. The two alloys have different processing conditions, from which several conditions, like the extrusion ratio, can influence this, but at least it can be concluded that the amount of cumulated strain during the cyclic aging did not significantly lower the fracture strain for any of the two alloys.

In conclusion, cyclic aging tests of a non-recrystallized AlMgSi alloy have been conducted on a flat extruded profile with orthotropic symmetry and a corresponding rolling type of texture and on a round profile with axi-symmetry and a corresponding fiber texture. The cumulative plastic strain was found to be significantly larger for the flat extrusion with orthotropic symmetry. It is likely that the symmetry of the slip systems of the ⟨100⟩ and ⟨111⟩ fibers during the cyclic aging is the main reason for this. Even though the cumulated plastic strain is large, the local fracture strain in tensile tests is similar as in the peak aged condition and a significant degree of diffuse necking was found for both textures. The early slant fracture observed in AlZnMg alloys in the cyclic aged condition, is not seen for the AlMgSi alloy investigated here.

Data availability

The raw data from the experiments conducted is available on the Zenodo Repository http://doi.org/10.5281/zenodo.10108981.

CRediT authorship contribution statement

Akash Gopal: Conceptualization, Writing – original draft, Data curation, Visualization, Investigation. **Sohail Shah:** Conceptualization, Data curation, Writing – review & editing. **Bjørn Holmedal:** Conceptualization, Writing – original draft.

Declaration of competing interest

The authors declare that they do not hold any competing interest that may have affected the work reported here.

Acknowledgement

The authors would like to thank Benteler Automotive Raufoss and Norsk Hydro Aluminium for providing the materials used in this work and Marie R. Sørlie and Håkon Linga for measuring the pole figures.

References

[1] X.L. Chen, E.A. Mortsell, J.K. Sunde, O. Minho, C.D. Marioara, R. Holmestad, E. Kobayashi, Enhanced mechanical properties in 6082 aluminum alloy processed by cyclic deformation, Metals (Basel) 11 (11) (2021) 1735.
[2] C.R. Hutchinson, F. de Geuser, Y. Chen, A. Deschamps, Quantitative measurements of dynamic precipitation during fatigue of an Al-Zn-Mg-(Cu) alloy using small-angle X-ray scattering, Acta Mater. 74 (2014) 96–109.
[3] S.H. Shah, A. Gopal, E. Thronsen, C. Hatzoglou, B. Holmedal, Precipitation, mechanical properties and early slant ductile fracture in cyclic and naturally aged Al-Zn-Mg(-Cu) alloys, Mater. Des. 222 (2022) 111026.
[4] S.H. Shah, E. Thronsen, C. Hatzoglou, S. Wenner, C.D. Marioara, R. Holmestad, B. Holmedal, Effect of cyclic ageing on the early-stage clustering in Al-Zn-Mg(-Cu) alloys, Mater. Sci. Eng. A 846 (2022) 143280.
[5] W.W. Sun, Y.M. Zhu, R. Marceau, L.Y. Wang, Q. Zhang, X. Gao, C. Hutchinson, Precipitation strengthening of aluminum alloys by room-temperature cyclic plasticity, Science 363 (6430) (2019) 972–975.
[6] N. Chung, J.D. Embury, J.D. Evensen, R.G. Hoagland, C.M. Sargent, Unstable shear failure in a 7075 aluminum-alloy, Acta Metall. 25 (4) (1977) 377–381.